

Decomposition of indigo carmine solution by ozone bubble pulsed discharge: Effect of the number of electrode pairs and injected ozone gas concentration

Soichiro Yamaguchi¹, Taichi Oyama², Ryosuke Nakano², Naoki Osawa^{2,*}, Yoshio Yoshioka²

¹ Graduate Program in Electrical and Electronic Engineering, Kanazawa Institute of Technology, Ishikawa, Japan

² Department of Electrical and Electronic Engineering, Kanazawa Institute of Technology, Ishikawa, Japan

* Corresponding author: n.osawa@neptune.kanazawa-it.ac.jp (Naoki Osawa)

Received: 12 November 2019

Revised: 14 April 2020

Accepted: 17 April 2020

Published online: 25 April 2020

Abstract

We developed a continuous water treatment system consisting of an ozone generator, an ejector nozzle, and a pulsed discharge device. We confirmed that the synergistic effect on indigo carmine decomposition by a combination of ozone injection and electrical discharge exists. In this paper, in order to maximize the synergistic effect, we investigated the effect of the number of electrode pairs and injected ozone gas concentration on indigo carmine decomposition. The results obtained are as follows; (1) discharge energy did not change, when we change the number of electrode pairs. However, average power increased with increasing the number of electrode pairs due to the increase in discharge probability. Large number of electrode pairs leads to a positive effect on indigo carmine decomposition, (2) the synergistic effect increased with increasing injected ozone gas concentration, (3) the reduction of ozone bubble size and the increase of the number of ozone bubbles by pulsed discharge generation is not the cause of the increase of synergistic effect, and (4) we confirmed that the amount of OH (309 nm), H_α (656 nm) and O (777 nm) increased with increasing injected ozone gas concentration. This result suggested that the increase of radical generation from the ozone molecule by pulsed discharge is the cause of the increase of synergistic effect.

Keywords: Ozone, OH radical, O radical, ozone bubble pulsed discharge, indigo carmine decomposition.

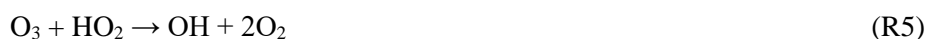
1. Introduction

In a plasma based advanced oxidation process (plasma AOP), hydroxyl (OH) radicals of highly oxidizing agent are generated by plasma in the water [1]. It is well known that OH radicals are generated by electron bombardment of water molecules and/or reacting oxygen (O) radicals with water molecules. OH radicals can decompose persistent organics that cause water pollution [2]. Therefore, the plasma AOP is a promising technology for the treatment of drinking water and industrial wastewater [3, 4]. Since the radicals are highly reactive (a short lifetime), radicals may disappear before reacting with persistent organics.

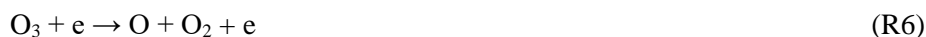
So far, many researchers have investigated the plasma AOP system. They reported several kinds of OH radical generation method, e.g. pulsed discharge along the water surface [5], dc discharge inside bubbles in water [6], underwater discharge [7], dielectric barrier discharge (DBD) with mist [8], pulsed DBD in a gas-liquid two-phase flow [9], and nanosecond pulse discharges at a liquid/vapor interface [10]. In these papers, production reactions of OH radicals were proposed as follows:



Furthermore, under O₃ coexistence condition, OH radicals are produced by this reaction.



In general, O radicals are produced by electron impact and/or thermal decomposition of O₃:



These reactions suggested that if we apply a combination of ozone injection and electrical discharge to the plasma AOP, the production of OH radicals will be enhanced. In order to verify the hypothesis, we developed a continuous water treatment system consisting of an ozone generator, an ejector nozzle, and a pulsed discharge device [11]. The results that we obtained were as follows; (1) in the case of Air Bubble Pulsed Discharge (ABPD), the existence of OH radicals and O radicals was observed by an optical emission spectroscopy, and we confirmed that these radicals reacted with indigo carmine, (2) in the case of Ozone Bubble Pulsed Discharge (OBPD), the existence of OH radicals and O radicals was also observed, and (3) the amount of indigo carmine decomposition by OBPD was larger than the sum of the amounts of indigo carmine decomposition by the ozone treatment alone and by the ABPD alone. From these results, we confirmed that the synergistic effect by a combination of ozone injection and electrical discharge exists. In order to maximize the synergistic effect, we considered that discharge device configuration and ozone gas concentration are important. Therefore, we changed both the number of electrode pairs and the injected ozone gas concentration, and investigated the rate of indigo carmine decomposition.

2. Experimental setup

2.1 Ozone bubble pulsed discharge system

Fig. 1 shows an experimental setup. The system consists of an ozone generator, an ejector nozzle, a pump, a pulsed power source, and a pulsed discharge device. Ozone was generated with a DBD device filled with glass beads (beads size: 6 mm). AC high voltage was applied to the ozone generator by an inverter power source (4210, NF corporation) and a step-up transformer (YHT-15K-0.5K, Yamabishi Electric). The applied voltage (V) of the ozone generator was measured by a high voltage probe (EP-50K, Nisshin Pulse Electronics).

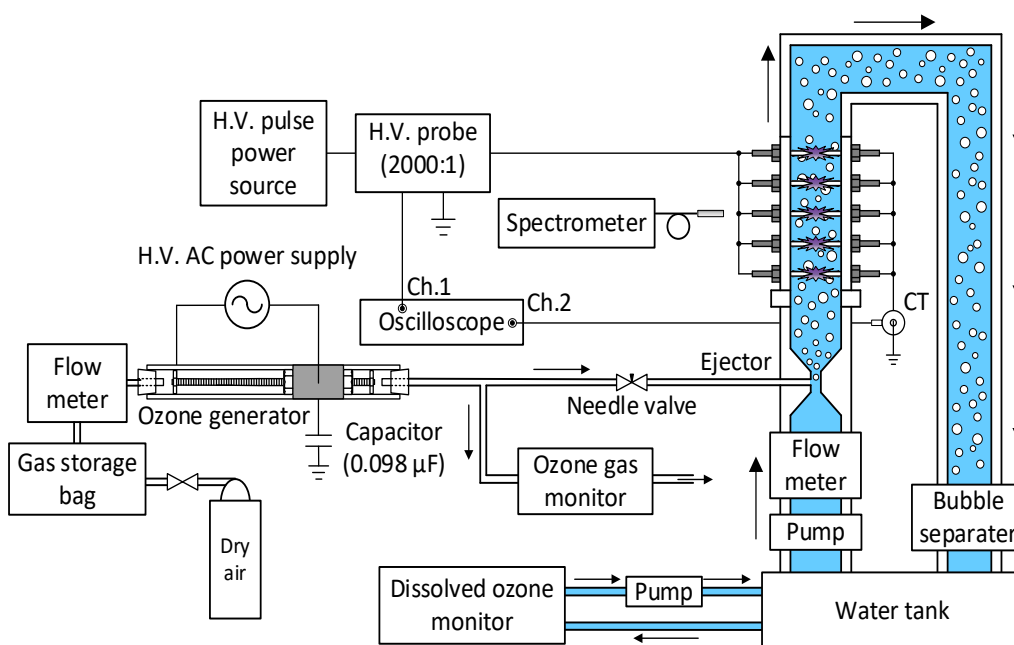


Fig. 1. Experimental setup

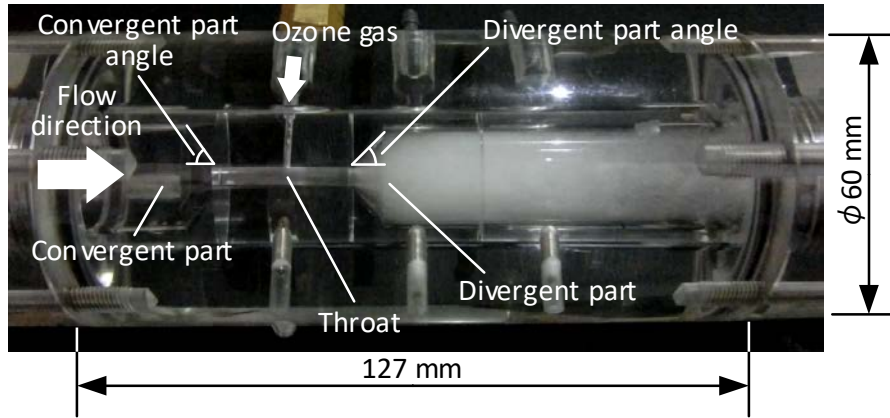


Fig. 2. Picture of ejector nozzle.

The charge (q) was measured by the voltage drop across an integral capacitor ($0.098 \mu\text{F}$). Discharge power of the ozone generator was calculated by multiplying the area of V-q Lissajous figure by power frequency. The ozone gas concentration was measured by an UV absorption type ozone monitor (EG-3000B/01, Ebara Jitsugyo). Dry air (absolute humidity: 119.3 mg m^{-3}) was used as a source gas of the ozone generator. The gas flow rate of the ozone generator was adjusted to 2.0 L min^{-1} by a needle valve.

In order to generate running water, a pump was connected to the upstream side of the ejector nozzle. Ozone bubbles were injected to the running water by the ejector nozzle. The geometry of the nozzle was shown in Fig. 2. The throat diameter is set to 3 mm. Convergent and divergent part angles were set to 60° and 45° , respectively. The indigo carmine solution was circulated in the system. A pair of needle electrodes was placed at 120 mm downstream of the gas suction port of the ejector nozzle. The maximum pairs of needle electrodes were 5. Electrodes were spaced 20 mm apart. The gap length of the needle electrode was fixed to 2 mm. The pulsed voltage was generated by a magnetic pulse compression type pulsed power supply (MPC3010S-50SP, Suematsu Electronics). The applied voltage and current were measured by a high voltage probe (EP-50K, Nisshin Pulse Electronics) and a high frequency CT (model 2877, Pearson Electronics) with a shunt to extend the range. The voltage and current waveform were measured by an oscilloscope (TBS2104, 100MHz, 1GS/s, Tektronix). A discharge probability (η) was calculated by measuring the number of pulsed discharge occurrence and the number of pulsed voltage application. The discharge probability (η), energy for pulsed discharge (E_p) and the average power for pulsed discharge (P_p) was calculated by Eqs. (1)- (3).

$$\eta = \frac{N_1}{N_2} \quad (1)$$

$$E_p = \int v(t) \times i(t) dt \quad (2)$$

$$P_p = \eta \times f \times E_p \quad (3)$$

Here, N_1 is the number of discharge occurrence, N_2 is the number of pulsed voltage application, $v(t)$ [V] is an instantaneous voltage at t [s], $i(t)$ [A] is an instantaneous current at t [s], and f [pps] is a pulse repetition rate, respectively. Detailed experimental conditions are summarized in Table 1 and 2.

Table 1. Experimental conditions for ozone generator.

Parameters	Value
Flow rate of air [L min^{-1}]	2.0
Applied voltage [kV]	12.8, 14.3, 14.7
Frequency [Hz]	340, 400, 540
Discharge power [W]	8.0, 9.9, 14.2
Ozone concentration [ppm]	700, 1000, 1300

Table 2. Experimental conditions for pulsed discharge device.

Parameters	Value
Applied voltage [kV]	30
Repetition rate [pps]	300

2.2 Decomposition conditions of indigo carmine solution

Firstly, in order to clarify the effect of the number of electrode pairs on indigo carmine decomposition, the amount of decomposition by the 1 electrode pair system was compared with that by the 5 electrode pairs system. Secondly, in order to clarify the effect of ozone injection and simultaneous application of pulsed discharge on indigo carmine decomposition, injected ozone gas concentration was changed as shown in Table 1. In this experiment, we used tap water of pH 7.6 and conductivity 212–262 $\mu\text{S cm}^{-1}$. Detailed decomposition conditions are summarized in Table 3.

Table 3. Treatment conditions for indigo carmine.

Parameters	Value
Flow rate of water [L min^{-1}]	7.3
Initial concentration of indigo carmine [mg L^{-1}]	38
Volume of solution [L]	3.0

2.3 Calculation of indigo carmine decomposition rate

The amount of indigo carmine decomposition was quantified from the absorbance spectra at 612 nm using a visible spectrophotometer (ASV11D, ASONE) and calibration curve. The detection limit is 0.27 mg L^{-1} . The decomposition rate α [%] was calculated by Eq. (4).

$$\alpha = \frac{c_0 - C(t)}{c_0} \times 100 \quad (4)$$

Here, C_0 [mg L^{-1}] is the initial concentration of indigo carmine solution and $C(t)$ [mg L^{-1}] is the instantaneous concentration of indigo carmine solution at t [s].

3. Results

3.1 Effect of the number of electrode pairs on discharge characteristics and indigo carmine decomposition

Fig. 3 and Fig. 4 show typical voltage and current waveforms of the 1 electrode pair system and the 5 electrode pairs system in the running water with air bubbles. The applied voltage and the repetition rate were set to 30 kV and 300 pps, respectively. From these figures, it is seen that almost no current flows in the running water before discharge occurs even though the voltage is increasing. Therefore, we concluded that the energy consumption at water is negligible. From Fig. 3, it is seen that the rise time of pulsed voltage was 0.22 kV ns^{-1} and the maximum current was 292 A. Discharge probability for 1 electrode pair system was 63%. The discharge energy and average power were 123 mJ and 23 W, respectively. On the other hand, from Fig. 4, it is seen that the rise time of pulsed voltage was 0.23 kV ns^{-1} and the maximum current was 273 A. Discharge probability for 5 electrode pairs system was 94%. The discharge energy and the average power were 129 mJ and 36 W, respectively.

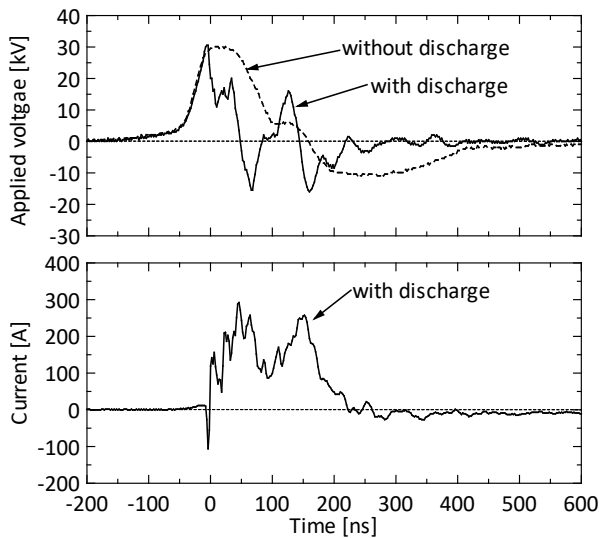


Fig. 3. Voltage and current waveform by 1 electrode pair system.

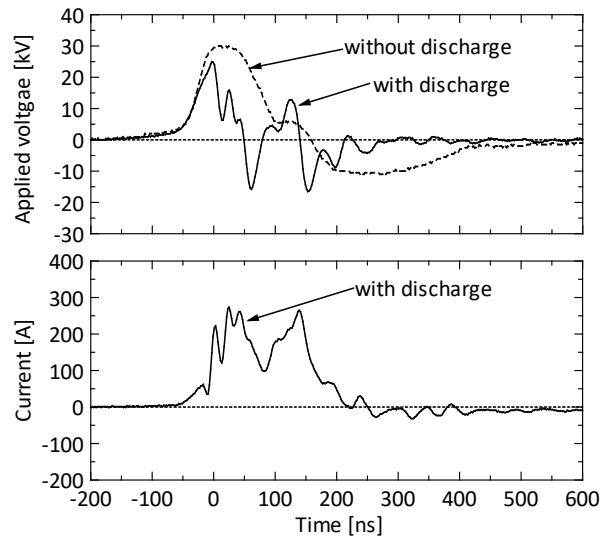
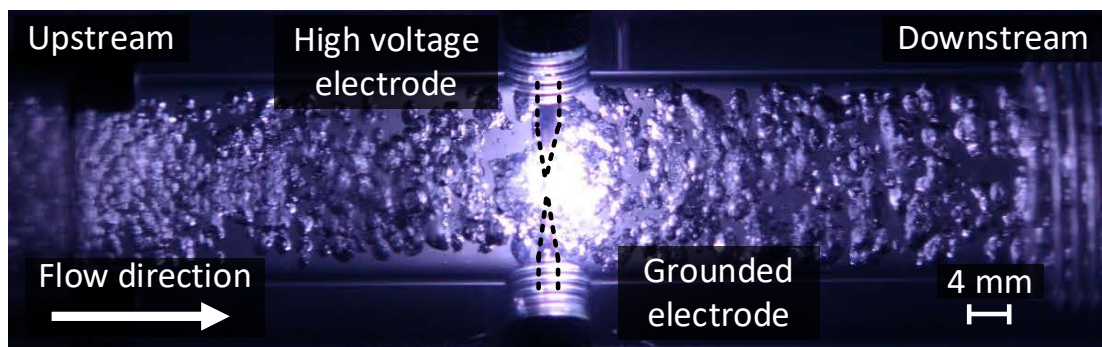
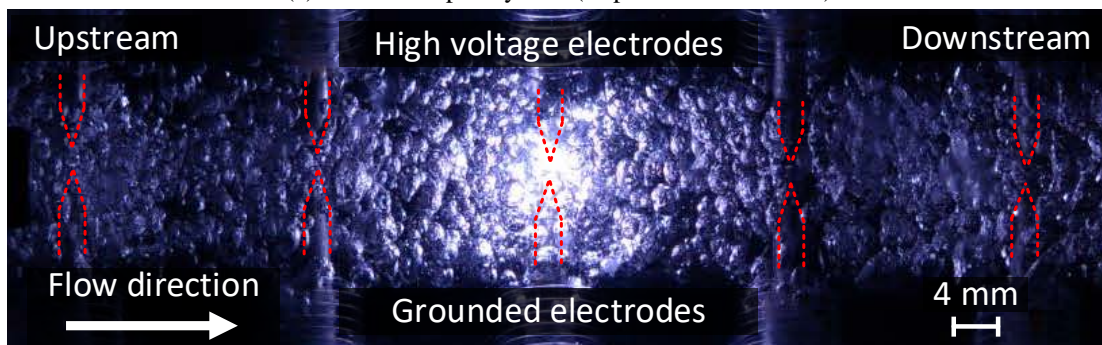


Fig. 4. Voltage and current waveform by 5 electrode pairs system.

Fig. 5 shows examples of discharge photographs. Since exposure time was set to 2 ms for 5 electrode pairs system or 2.5 ms for 1 electrode pair system which is shorter than the pulse voltage repetition time (3.3 ms), a discharge photograph was taken when one pulse voltage is applied. From these photographs, we confirmed that a single discharge appeared between needle electrodes despite the 5 electrode pairs system. Since the discharge appearance was the same in both electrode systems, the discharge energy was almost same in both electrode systems. However, the average power was different. This is because when the number of electrode pairs increases, the probability for the bubbles in the water to fill the gaps between the electrodes becomes high. Since dielectric strength for air is lower than that for water, this phenomenon will lead to a higher discharge probability. In order to clarify this phenomenon, further investigation by a high-speed observation is necessary.



(a) 1 electrode pair system (Exposure time: 2.5 ms)



(b) 5 electrode pairs system (Exposure time: 2 ms)

Fig. 5. Discharge photographs.

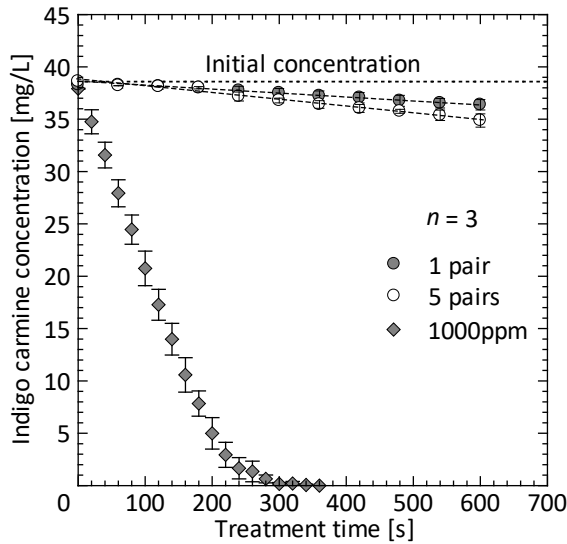


Fig. 6. Temporal change of indigo carmine concentration with ABPD and ozone injection alone.

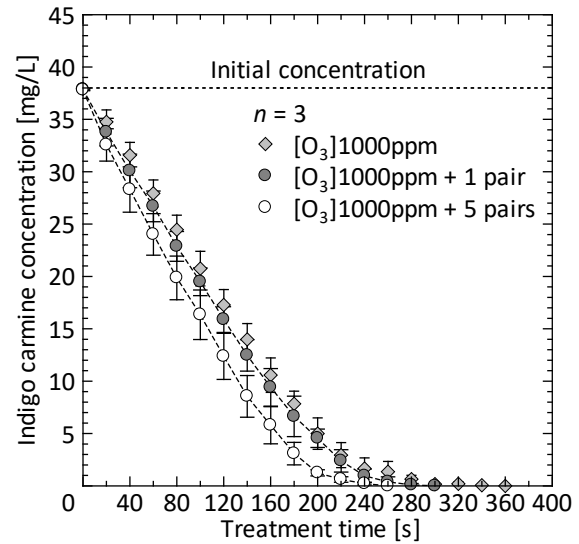


Fig. 7. Temporal change of indigo carmine concentration with OBPD in 1 pair and 5 pairs.

Fig. 6 shows temporal change of indigo carmine concentration by ABPD and ozone injection alone. Here, n is experimental times and error bars show standard deviation. Indigo carmine concentration decreased with increasing treatment time. It is seen that indigo carmine concentration in the 5 electrode pairs system decreased a bit faster than that in the 1 electrode pair system. Although the indigo carmine solution was treated for 600 s with the ABPD treatment, indigo carmine concentration did not reach less than a detection limit. Indigo carmine concentration at 100 s by 1 electrode pair system and by 5 electrode pairs system were 37.6 mg L^{-1} and 37.1 mg L^{-1} respectively. From these results, we confirmed that the effect of the number of electrode pairs in ABPD treatment is small for indigo carmine decomposition. On the other hand, in the case of 1000ppm ozone treatment alone, indigo carmine concentration drastically decreased with increasing treatment time and it reached to less than the detection limit around 360 s. Indigo carmine concentration at 100 s was 20.75 mg L^{-1} . We confirmed that the decomposition effect by ozone injection treatment alone was higher than that of by ABPD treatment.

Next, we investigated the effect of ozone injection and simultaneous application of pulsed discharge. Fig. 7 shows temporal change of indigo carmine concentration with the OBPD in 1 electrode pair and 5 electrode pairs systems. Indigo carmine concentration drastically decreased with increasing treatment time and it reached to less than the detection limit at around 260 s. At the same time, indigo carmine concentration with the 5 electrode pairs system was clearly lower than that of the 1 electrode pair system. Indigo carmine concentration at 100 s for the 1 electrode pair system and for the 5 electrode pairs system were 19.49 mg L^{-1} and 16.35 mg L^{-1} , respectively. From these results, we confirmed that the number of electrode pairs is effective to increase the decomposition rate of indigo carmine by OBPD treatment.

3.2 Effect of injected ozone gas concentration on OBPD treatment

In order to clarify the effect of injected ozone concentration on OBPD treatment, firstly, we investigated the decomposition effect by ozone injection treatment alone. Fig. 8 shows temporal change of indigo carmine concentration by ozone injection treatment alone. We confirmed that the indigo carmine concentration became lower when ozone gas with higher ozone concentration was injected. Indigo carmine concentrations at 100 s on various injected ozone gas concentration were summarized as Table 4.

Table 4. Effect of ozone injection treatment alone on indigo carmine concentration at 100 s.

Injected ozone concentration [ppm]	Indigo carmine concentration [mg L^{-1}]
700	25.32
1000	20.75
1300	16.55

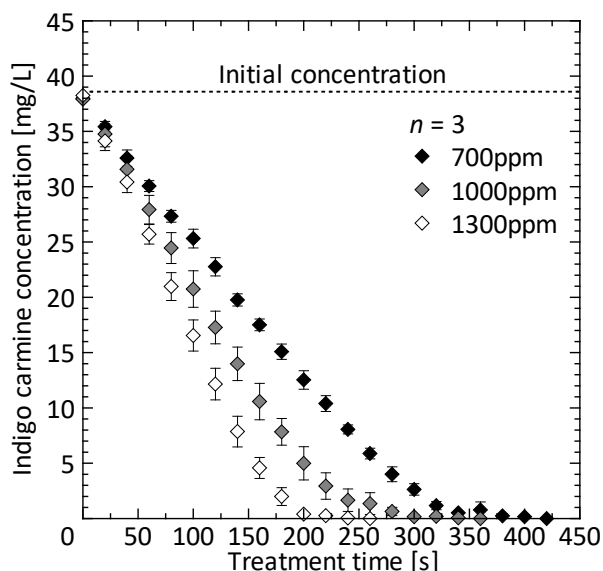


Fig. 8. Temporal change of indigo carmine concentration by ozone injection treatment alone.

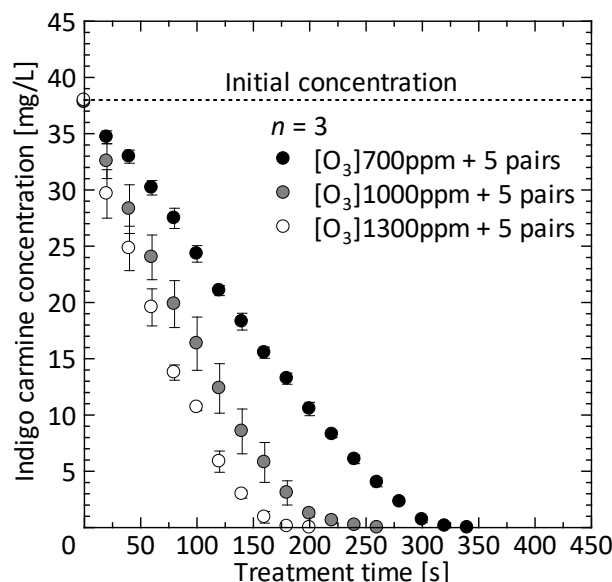


Fig. 9. Temporal change of indigo carmine concentration by OBPD treatment.

Fig. 9 shows temporal change of indigo carmine concentration by OBPD treatment with 5 electrode pairs system. The test result showed that the indigo carmine concentration decreased with increasing injected ozone gas concentration. Indigo carmine concentrations at 100 s on various injected ozone gas concentration were summarized as Table 5.

The decrease of indigo carmine concentration was calculated by subtracting the concentration at 100 s which is summarized in Table 4 and 5 from the initial concentration. The decrease of indigo carmine concentration at 100 s by ABPD treatment with 5 electrode pairs system alone and by 1300 ppm ozone injection treatment alone were 0.9 mg L⁻¹ and 21.45 mg L⁻¹, respectively. Therefore, the sum of these treatments was 22.35 mg L⁻¹. However, the decrease of indigo carmine concentration at 100 s by 1300 ppm OBPD treatment was 27.31 mg L⁻¹. Therefore, it is obvious that the synergistic effect exists in the OBPD treatment. Next, we calculated the synergistic effect of OBPD treatment.

Table 5. Effects of ABPD and OBPD treatment on indigo carmine concentration at 100 s.

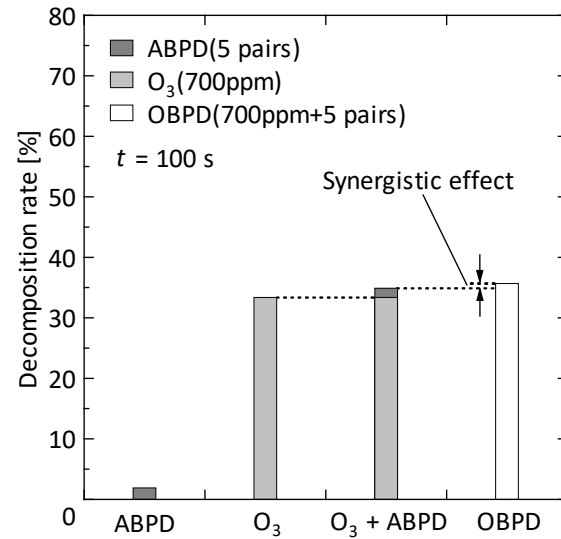
Ozone concentration [ppm]	Indigo carmine concentration [mg L ⁻¹]	Remarks
0	37.10	by ABPD
700	24.32	by OBPD
1000	16.35	by OBPD
1300	10.69	by OBPD

Table 6. Calculation result of synergistic effect of OBPD on indigo carmine concentration at 100 s.

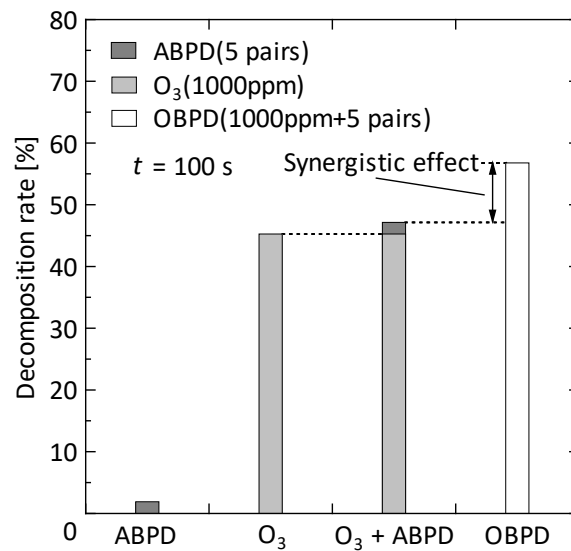
Ozone concentration [ppm]	Synergistic effect [%]
700	0.78
1000	9.6
1300	13.21

3.2 Calculation of synergistic effect by OBPD treatment

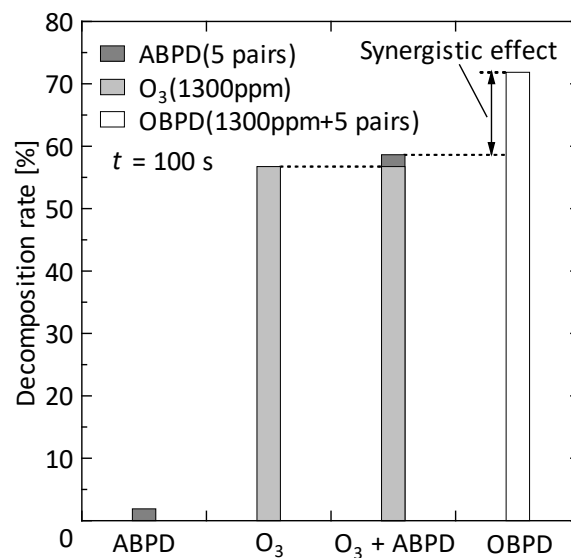
In order to confirm the synergistic effect by OBPD treatment, the decomposition rates for 100 s treatment time by 5 electrode pairs system were analyzed. Fig. 10 shows the analysis result of the synergistic effect of OBPD treatment. In all conditions, the decomposition rate of OBPD treatment was higher than the sum of the decomposition rates of ABPD treatment and ozone injection treatment alone. Synergistic effect of various ozone concentrations was summarized in Table 6. From Table 6, we found that synergistic effect increased with increasing ozone concentration.



(a) ozone concentration: 700ppm



(b) ozone concentration: 1000ppm



(c) ozone concentration: 1300ppm

Fig. 10. Analysis result of synergistic effect by OBPD treatment on indigo carmine decomposition.

4. Discussion

4.1 Dissolved ozone concentration

It is reported that the shock wave generated by pulsed discharge inside bubbles collapses bubbles themselves and the resultant smaller bubbles increases a specific area [11, 12]. The large specific area enhances the ozone mass transfer from bubbles to the water [13]. Therefore, if the ozone gas bubble size becomes small by pulsed discharge, dissolved ozone concentration will increase and therefore subsequent decomposition of indigo carmine is considered to be increased. In order to confirm this idea, we measured dissolved ozone concentration by a UV absorption type dissolved ozone monitor (EL-600, Ebara Jitsugyo). In order to avoid interference caused by the bubbles in water, we used a bubble separator. In the separator, bubbles in the running water are removed by swirling flow. In this experiment, we used tap water without indigo carmine.

Fig. 11 shows the relation between injected ozone gas concentration and dissolved ozone concentration. Dissolved ozone concentration increased with increasing injected ozone gas concentration. We confirmed that the dissolved ozone concentration by OBPD treatment was lower than that of by ozone injection treatment alone at the same injected ozone gas concentration. This is because ozone in the bubbles and dissolved ozone was decomposed by pulsed discharge. These results suggested that the dissolved ozone concentration increase by pulsed discharge is not the cause of the increase of synergistic effect.

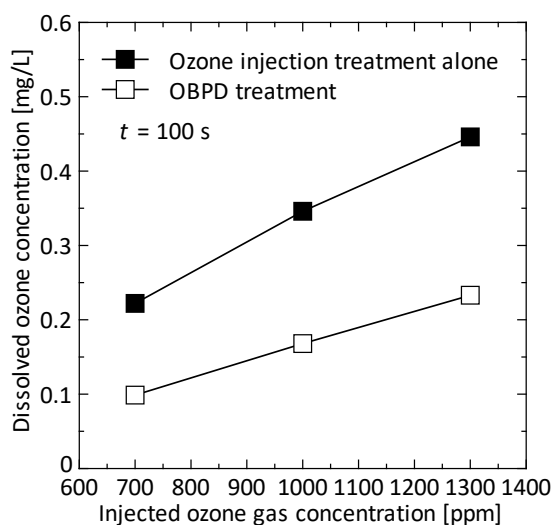


Fig. 11. Relation between injected ozone gas concentration and dissolved ozone concentration. (effect of pulsed discharge application).

4.2 Reactive species generated by pulsed discharge

We confirmed that when the ozone concentration increased in the OPBD treatment, the synergistic effect enhanced. We are thinking that the amount of reactive species generated by pulsed discharge was increased by increasing injected ozone gas concentration. Here, in the case of OBPD treatment, for example, reactions (R1) – (R7) and following radical generation reactions occur [4, 6, 7, 14].



In order to confirm this, the emission spectra of pulsed discharge were observed by a compact multichannel spectrometer (USB4000, Ocean Optics). In this experiment, we used tap water without indigo carmine. Measuring conditions were summarized in Table 7.

Fig. 12 shows optical emission spectra for OBPD. OH (309 nm), H α (656 nm) and O (777 nm) were detected. Fig. 13 shows optical emission spectra for OBPD by various ozone concentration. Intensities for O,

OH and H_{α} increased with increasing injected ozone gas concentration. These radicals contribute to indigo carmine decomposition despite dissolved ozone concentration decreased by pulsed discharge. These results suggested that the increase of radical generation from the ozone molecule by pulsed discharge is the cause of the increase of synergistic effect. In this experiment, we used air as the source gas of the ozone generator. Therefore, OH radicals were generated by reacting reactive oxygen and nitrogen species (RONS). We could not distinguish the effects of ROS and RNS on indigo carmine decomposition from optical emission spectra. Further study on OBPD treatment using ozone generated by changing the admixture ratio of N_2 and O_2 in a source gas experiment is necessary.

Table 7. Measuring conditions for optical emission spectroscopy.

Settings	Value
Exposure time [ms]	200
Averaging	20
Slit width [μm]	200
Number of lines [lines/mm]	600
Distance between plasma to optical fiber input [mm]	140

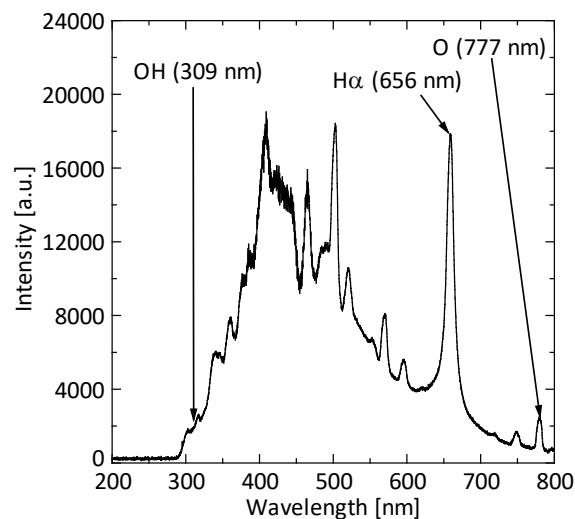


Fig. 12. Observation of optical emission in OBPD with 1000ppm ozone injection.

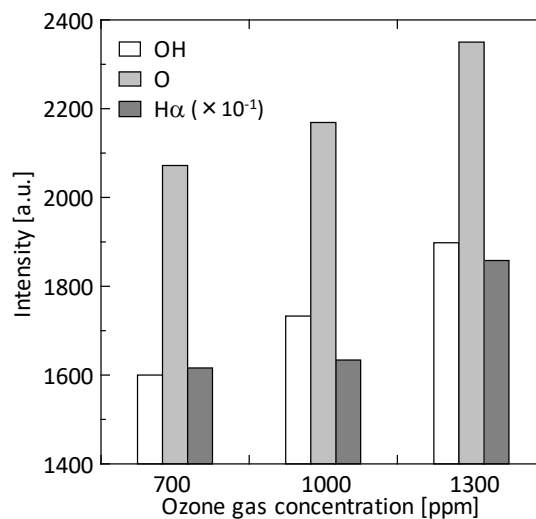


Fig. 13. Optical emission spectra for OBPD by various ozone concentration.

5. Conclusion

In this paper, we investigated the effect of the number of electrode pairs and injected ozone gas concentration, in order to maximize the synergistic effect by OBPD treatment. The results obtained are as follows:

- (1) Discharge energy did not change, when we change the number of electrode pairs. However, Average power was increased with increasing the number of electrode pairs due to the increase in discharge probability. Namely large number of electrode pairs leads to a positive effect on the synergistic effect.
- (2) The synergistic effect increased with increasing injected ozone gas concentration.
- (3) The reduction of ozone bubble size and the increase of the number of ozone bubble by pulsed discharge generation is not the cause of the increase of synergistic effect on indigo carmine decomposition.
- (4) In the case of OBPD treatment, OH (309 nm), H α (656 nm) and O (777 nm) were detected and they increased with increasing ozone concentration. This result suggested that the increase of radical generation from the ozone molecule by pulsed discharge is the cause of the increase of synergistic effect.

Acknowledgment

We would like to express my gratitude to Prof. K. Aizawa of Kanazawa Institute of Technology for support on optical emission spectroscopy.

References

- [1] Takeuchi N., Ishibashi N., Sugiyama T. and Kim H.H., Effective utilization of ozone in plasma based advanced oxidation process, *Plasma Sources Sci. Technol.*, Vol.27 (5), pp. 055013, 2018.
- [2] Yamatake A., Fletcher J., Yasuoka K., and Ishii S., Water treatment by fast oxygen radical flow with DC-driven microhollow cathode discharge, *IEEE Trans. Plasma Sci.*, Vol.34 (4), pp. 1375–1381, 2006.
- [3] Nakagawa Y., Ono R., and Oda T., Effect of discharge polarity on OH density and temperature in coaxial-cylinder barrier discharge under atmospheric pressure humid air, *Jpn. J. Appl. Phys.*, Vol. 57 (9), pp. 096103, 2018.
- [4] Nani L., Tampieri F., Ceriani E., Marotta E. and Paradisi C., ROS production and removal of the herbicide metolachlor by air non-thermal plasma produced by DBD, DC⁻ and DC⁺ discharges implemented within the same reactor, *J. Phys. D: Appl. Phys.*, Vol. 51 (27), pp. 274002, 2018.
- [5] Takeuchi N., Ando M., and Yasuoka K., Investigation of the loss mechanisms of hydroxyl radicals in the decomposition of organic compounds using plasma generated over water, *Jpn. J. Appl. Phys.*, Vol.54 (11), pp. 116201, 2015.
- [6] Takeuchi N., Ishii Y. and Yasuoka K., Modelling chemical reactions in dc plasma inside oxygen bubbles in water, *Plasma Sources Sci. Technol.*, Vol. 21 (1), pp. 015006, 2012.
- [7] Hayashi H., Akamine S., Ichiki R., and Kanazawa S., Comparison of OH radical concentration generated by underwater discharge using two methods, *Int. J. Plasma Environ. Sci. Technol.*, Vol.10 (1), pp. 24–28, 2016.
- [8] Shibata T. and Nishiyama H., Water treatment by dielectric barrier discharge tube with vapor flow, *Int. J. Plasma Environ. Sci. Technol.*, Vol.11 (1), pp. 112–117, 2017.
- [9] Matsui Y., Takeuchi N., Sasaki K., Hayashi R. and Yasuoka K., Experimental and theoretical study of acetic-acid decomposition by a pulsed dielectric-barrier plasma in a gas–liquid two-phase flow, *Plasma Sources Sci. Technol.*, Vol. 20 (3), pp. 034015, 2011.
- [10] Winters C., Petrishchev V., Yin Z., Lempert W. R. and Adamovich I. V., Surface charge dynamics and OH and H number density distributions in near-surface nanosecond pulse discharges at a liquid/vapor interface, *J. Phys. D: Appl. Phys.*, Vol.48 (42), pp. 424002, 2015.
- [11] Yamaguchi S., Taichi O., Nakano R., and Osawa N., Generation of pulsed discharges in running water including ozone gas bubbles and its effect on indigo carmine decomposition, *J. Institute of Electrostatics Jpn.*, Vol. 43 (2), pp. 84–89, 2019 (in Japanese).
- [12] Sommers B. S. and Foster J. E., Plasma formation in underwater gas bubbles, *Plasma Sources Sci. Technol.* Vol. 23 (1), pp. 015020, 2014.
- [13] Hu L. and Xia Z., Application of ozone micro-nano-bubbles to groundwater remediation, *J. Hazard. Mater.*, Vol. 342, pp. 446–453, 2018.
- [14] Kogelschatz U., Dielectric-barrier discharges: Their history, discharge physics, and industrial applications, *Plasma Chem. Plasma Process.*, Vol.23 (1), pp. 1–46, 2003.